Robust current-mode control of bridgeless single-switch SEPIC PFC converter

Humam Al-Baidhani[1,2], Abdullah Sahib[3]
[1]Department of Electrical Engineering, Wright State University, Dayton, USA
[2]Department of Computer Techniques Engineering, Faculty of Information Technology, Imam Ja'afar Al-Sadiq University, Baghdad, Iraq
[3]Department of Electronic and Communication Technologies, Technical Institute, Al-Furat Al-Awsat Technical University, Najaf, Iraq

Article Info

Article history:

Received Aug 19, 2022
Revised Feb 8, 2023
Accepted Feb 21, 2023

Keywords:

AC-DC converter
Bridgeless SEPIC
Current-mode control
DCM
Single-switch PFC

ABSTRACT

In this paper, the nonlinear model of the bridgeless single-switch AC-DC single-ended primary-inductor converter (SEPIC) in discontinuous conduction mode is derived. In addition, a robust control method is introduced to accommodate the variations in input voltage and load current. The current-mode controlled power converter is designed to operate in buck and boost modes. The proposed closed-loop SEPIC converter is simulated in MATLAB to validate the design approach. The current-mode control scheme is also compared with the conventional voltage-mode controller. It is confirmed that the proposed control scheme exhibits precise tracking performance and enhanced transient response under large disturbances.

Corresponding Author:

Humam Al-Baidhani
Department of Electrical Engineering, College of Engineering and Computer Science
Wright State University
Dayton, OH 45435, USA
Email: al-baidhani.2@wright.edu

1. INTRODUCTION

In recent years, power factor correction (PFC) technique has been utilized with various power converter typologies. The AC-DC converters are highly demanded in several applications, such as uninterruptible power supplies, personal computers, and EV on-board chargers [1]. Modern power grids require power conversion stages with low total harmonic distortion (THD) and high-power factor [2]–[4]. In [5], [6], bridgeless AC-DC boost PFC converters have been introduced as alternatives for full-bridge AC-DC power converters to minimize conduction loss in bridge power diodes. However, due to the boost converter's structure, they are not applicable to low-voltage power demands.

The AC-DC bridgeless Cuk and SEPIC PFC converters have also been introduced to operate in buck and boost modes. Proportional-integral (PI) control [7] and current-mode control [8] schemes have been presented for bridgeless Cuk converters. The SEPIC PFC converters in [9]–[16] are designed to work in discontinuous conduction mode (DCM) to gain some advantages, such as zero-current turn-on in switches and zero-current turn-off in output diode. Other researchers have introduced the single-ended primary-inductor converter (SEPIC) PFC converter in continuous conduction mode (CCM) [17]–[19] and critical conduction mode (CRM) [20] depending on the design requirements and the control strategy. In [9]–[11], a bridgeless SEPIC PFC rectifier has been designed to achieve unity power factor and reduced THD. Furthermore, bridgeless SEPIC and Cuk PFC rectifiers with low conduction and switching losses have been introduced in [12]. A bridgeless isolated AC-DC SEPIC converter is proposed in [13] for EV battery chargers. Despite the analysis and the design procedure of power converters in previous literature, the design of proper control schemes that maintain constant voltage under large disturbances has not been discussed. Moreover, the reported AC-DC converters require two switches, which complicate the control scheme and decreases the power converter efficiency.

Bridgeless PFC-modified SEPIC rectifier with extended gain, bridgeless SEPIC converter-based computer power supply, and hybrid switched-capacitor voltage-doubler SEPIC PFC rectifiers have been proposed in [14], [15], and [16], respectively. In CCM operation, a bridgeless SEPIC converter without circulating losses [17], a bridgeless SEPIC converter with averaged current-mode controller [18], and a bridgeless SEPIC converter for a brushless DC motor [19] have been studied. GaN-based zero-voltage-switching (ZVS) bridgeless dual-SEPIC rectifier with integrated inductors [20] have also been introduced. The aforementioned AC-DC power converters have been integrated with control schemes that regulate the output voltage during line and load disturbances, but the power converters have been designed to operate in either buck or boost mode. In other words, the capability of the previous control schemes has been studied for a single dc output voltage, which yields a power supply with a limited operating point. Another drawback with these power converters is the double-switch configuration, which degrades the power stage efficiency and increase the control circuit complexity.

Few research endeavors have presented the bridgeless single-switch SEPIC PFC converters to decrease the components count of the switching devices and simplify the control design. For example, a single-stage high power factor SEPIC PFC converter for light electric vehicles [21], a modified SEPIC converter for high-power-factor rectifier [22], and a single-switch bridgeless SEPIC PFC converter [23] have been introduced. However, the existing research endeavors have not yet considered robust control design of such type of power converters to maintain excellent tracking performance and accommodate the variations in input voltage and load current. Further, the previous current-mode control systems have comprised two PI compensators and three sensors for input voltage, output voltage, and inductor current. Hence, a simplified controller with minimal added components is required to reduce the complexity and implementation cost.

This research aims to design a simple current-mode control scheme for a bridgeless SEPIC PFC converter in discontinuous conduction mode. The closed-loop single-switch AC-DC power converter contains a PI compensator and two sensors for output voltage and input inductor current. The AC-DC power converter is designed to convert ac input voltage to dc output voltage under abrupt changes in input voltage and load current. The control law is designed to maintain robust tracking performance and wide operating range. The analysis and dynamics of the power converter are introduced. MATLAB/Simulink model is developed, and simulations are conducted to validate the control design method under steady-state and transient conditions.

2. DYNAMICS OF SEPIC CONVERTER IN DCM

The bridgeless AC-DC SEPIC converter circuit is shown in Figure 1(a). It is assumed that the SEPIC converter is operated in DCM, which results in three configurations as illustrated in Figures 1(b)-1(d). Initially, it has been assumed that the power converter starts with freewheeling mode, which means that the currents i_{L1} and i_{Lo} are constant.

The first configuration is shown in Figure 1(b), where Q_1 is ON and D_o is OFF. Using Kirchhoff's voltage and current laws, the dynamical equations can be derived, which give:

$$\left[L_1\frac{di_{L1}}{dt} \quad L_o\frac{di_{Lo}}{dt} \quad C_o\frac{dv_{Co}}{dt} \quad C_1\frac{dv_{C1}}{dt}\right]^T = \left[V_I \quad -v_{C1} \quad \frac{v_{Co}}{R_o} \quad -i_{Lo}\right]^T \tag{1}$$

in the second configuration, Q_1 is OFF and D_o is ON as shown in Figure 1(c). Using Kirchhoff's voltage and current laws, the power converter dynamics are:

$$\left[L_1\frac{di_{L1}}{dt} \quad L_o\frac{di_{Lo}}{dt} \quad C_o\frac{dv_{Co}}{dt} \quad C_1\frac{dv_{C1}}{dt}\right]^T = \left[V_I - v_{C1} - v_{Co} \quad v_{Co} \quad i_{Do} - \frac{v_{Co}}{R_o} \quad i_{Do} - i_{Lo}\right]^T \tag{2}$$

Figure 1(d) shows the third configuration, at which both Q_1 and D_o are turned OFF. The differential equations of the power converter in this configuration are expressed in (3).

$$\left[(L_1+L_o)\frac{di_{L1}}{dt} \quad (L_1+L_o)\frac{di_{Lo}}{dt} \quad C_o\frac{dv_{Co}}{dt} \quad C_1\frac{dv_{C1}}{dt}\right]^T = \left[V_I - v_{C1} \quad V_I - v_{C1} \quad \frac{v_{Co}}{R_o} \quad -i_{Lo}\right]^T \tag{3}$$

The nonlinear model of SEPIC converter is derived using the graphical method detailed in [24], which gives

$$\begin{bmatrix} \frac{di_{L1}}{dt} \\ \frac{di_{Lo}}{dt} \\ \frac{dv_{C1}}{dt} \\ \frac{dv_{Co}}{dt} \end{bmatrix} = \begin{bmatrix} \frac{V_I}{L_1}d_1 + \frac{(V_I - v_{C1} - v_{Co})}{L_1}d_2 + \frac{(V_I - v_{C1})}{L_1 + L_o}(1 - d_1 - d_2) \\ -\frac{v_{C1}}{L_o}d_1 + \frac{v_{Co}}{L_o}d_2 + \frac{(V_I - v_{C1})}{L_1 + L_o}(1 - d_1 - d_2) \\ \frac{1}{C_1}\left(i_{D_o} - i_{Lo}\right) \\ \frac{1}{C_o}\left(i_{D_o} - \frac{v_{Co}}{R_o}\right) \end{bmatrix} \tag{4}$$

The parameters d_1, d_2, and $1 - d_1 - d_2$ represent the time intervals during the first, second, and third configurations of SEPIC converter in DCM, respectively. According to [24], the diode current i_{D_o} and d_2 are

$$\begin{cases} i_{D_o} = \left(\frac{V_I}{L_1} + \frac{v_{C1}}{L_o}\right) d_1 d_2 T \\ d_2 = \frac{2(i_{L1} + i_{Lo})}{\left(\frac{V_I}{L_1} + \frac{v_{C1}}{L_o}\right) d_1 T} - d_1. \end{cases} \tag{5}$$

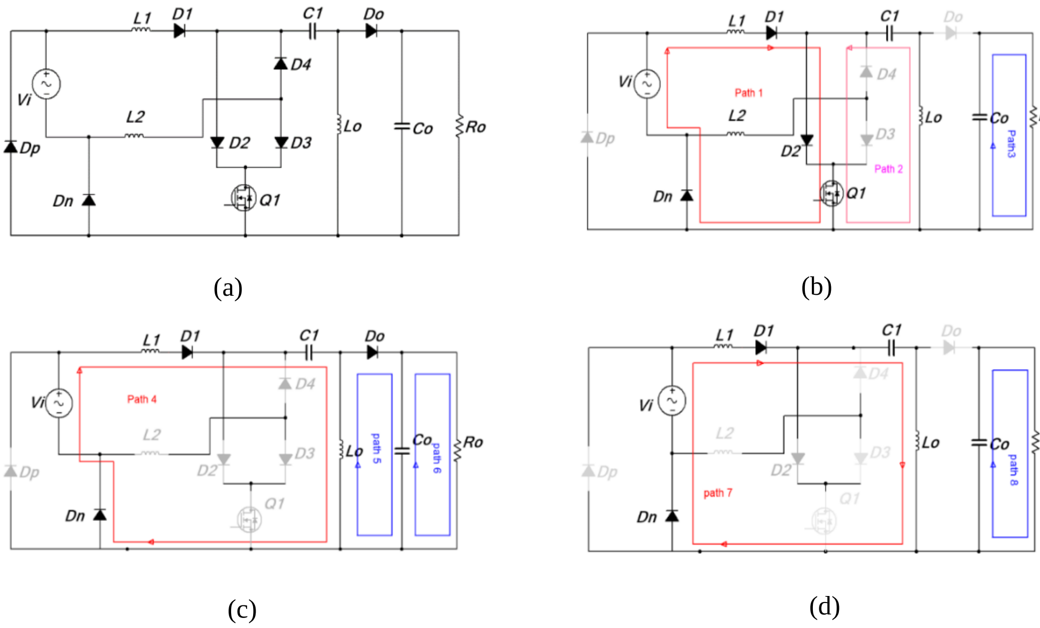

Figure 1. Single-switch power converter: (a) equivalent circuit, the configurations during positive half-line cycle when (b) Q_1 is ON and D_o is OFF, (c) Q_1 is OFF and D_o is ON, and (d) both Q_1 and D_o are OFF

3. PROPOSED CURRENT-MODE CONTROL SCHEME

The proposed current-mode control scheme consists of two loops, which are the outer voltage loop and inner current loop. The outer voltage loop contains the sensed output voltage, which is compared with a reference voltage V_r to generate a voltage error signal. The voltage error signal passes through a proportional-integral (PI) compensator to generate a reference inductor current I_R [8], which is defined as (6).

$$I_R = K_p(V_r - \beta v_o) + K_I \int (V_r - \beta v_o)dt. \tag{6}$$

The parameter β is the feedback network gain. The proportional gain K_p and integral gain K_I eliminate the tracking error of the output voltage and enhance the transient response characteristics. The gains can be chosen using Ziegler-Nichols method, where the gain values are tuned until the desired response is achieved.

However, since the SEPIC converter contains a right-half plane zero, the implementation of the voltage-mode controller yields slow response and undesirable transient characteristics. This issue can be solved using the averaged current-mode control method, which ensures a fast tracking for the reference current. The control method can be achieved using the inductor current i_{L1}. The rectified value of the current i_{L1} passes through the gain K [8]. The inner current loop is compared with the reference current I_R in (6) to generate the current-mode control law.

$$u = K_p(V_r - \beta v_o) + K_I \int (V_r - \beta v_o)dt - K|i_{L_1}| = I_R - K|i_{L_1}|. \quad (7)$$

The control law in (7) is a continuous function, where $u \in [0, 1]$. Hence, a pulse-width modulator is required to convert the continuous function u to a PWM signal, which operates the power converter at constant switching frequency [25], [26]. The Simulink model of the closed-loop power converter is shown in Figure 2. It is worth noting that the proposed current-mode controller is similar to the sliding-mode control method [27], which can be implemented using low-cost electronic circuit [28].

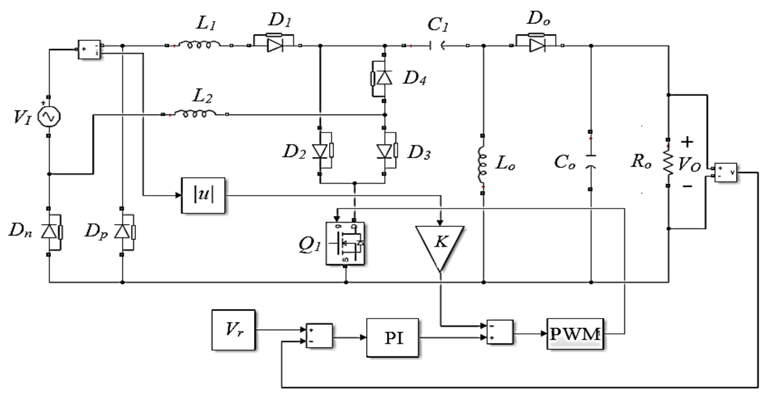

Figure 2. The Simulink model of the closed-loop AC-DC SEPIC converter

4. RESULTS AND DISCUSSION

4.1. Steady-state performance

The parameters of the bridgeless AC-DC SEPIC converter are shown in Table 1, which are selected according to the design procedure given in [16]. The proportional gain K_p, integral gain K_I, and inductor current gain K are 0.015, 1.45, and 0.042, respectively. The simulation results are depicted in Figure 3, which show the steady-state waveforms of the closed-loop bridgeless AC-DC power converter. It can be noticed that 120 VAC/60 Hz sinusoidal input voltage is converted to 48/220 VDC output voltage under nominal load resistance of 80 Ω. It has also been observed that the measured power factor is 0.99, whereas the output voltage ripple is less than 1%.

Table 1. Power converter parameters

Description	Parameter	Value	Description	Parameter	Value
Input inductor	L_1, L_2	4.4 mH	Input voltage	v_I	(80 - 160) VAC
Output inductor	L_o	100 µH	Input frequency	f	60 Hz
Input capacitor	C_1	1 µF	Output voltage	v_O	(48 - 220) VDC
Output capacitor	C_o	3.3 mF	Switching frequency	f_s	30 kHz
Load resistor	R_o	80 Ω			

4.2. Tracking and disturbance rejection

The characteristics of the closed-loop AC-DC power converter responses are summarized in Table 2. In buck mode, Figures 4(a) and 4(b) show the transient response under load disturbance, whereas Figures 4(c) and 4(d) show the output voltage response under line disturbance. As shown in Table 2, the largest percentage undershoot *PU* was 4%, while the longest settling time t_s was around 150 ms. It has also been observed that both disturbances are rejected, and the output voltage is maintained at 48 VDC.

Table 2. Characteristics of closed-loop SEPIC converter during line and load disturbances

Operation mode	Line/load disturbance	*PO*/*PU* (%)	t_s (ms)	V_O (V)
Buck	$v_I = 120 \rightarrow 160$ (V)	3.0	100	48
	$v_I = 120 \rightarrow 80$ (V)	4.0	150	
	$i_O = 0.6 \rightarrow 0.3$ (A)	2.7	150	
	$i_O = 0.3 \rightarrow 0.6$ (A)	3.0	120	
Boost	$v_I = 120 \rightarrow 160$ (V)	3	120	220
	$v_I = 120 \rightarrow 80$ (V)	3.6	150	
	$i_O = 2.75 \rightarrow 1.37$ (A)	3.4	250	
	$i_O = 1.37 \rightarrow 2.75$ (A)	3.6	150	

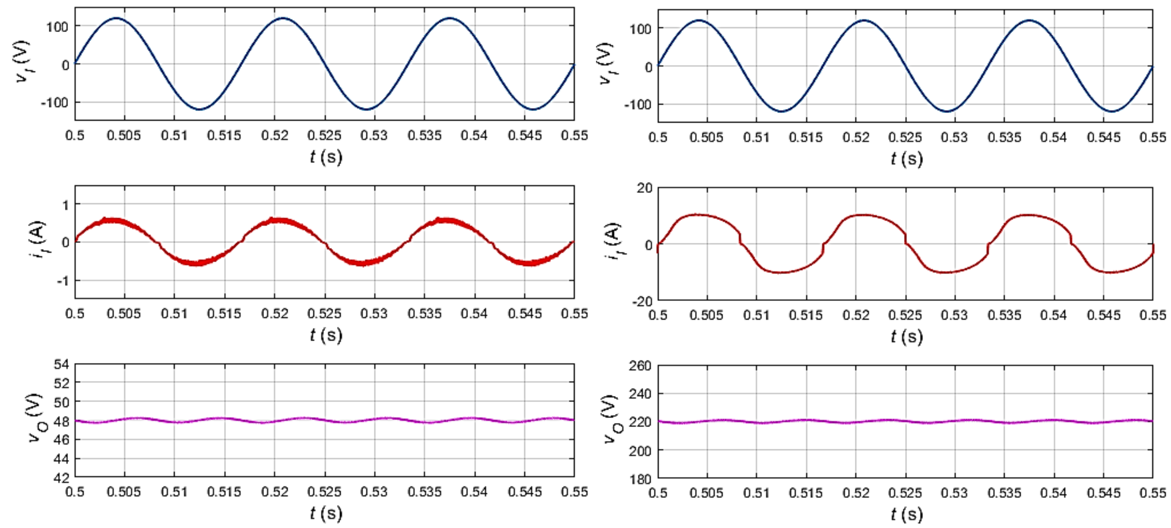

(a) (b)

Figure 3. Steady-state waveforms of bridgeless SEPIC converter in DCM. Input voltage v_I, input current i_I, and output voltage v_O in (a) buck mode (120 VAC to 48 VDC) and (b) boost mode (120 VAC to 220 VDC)

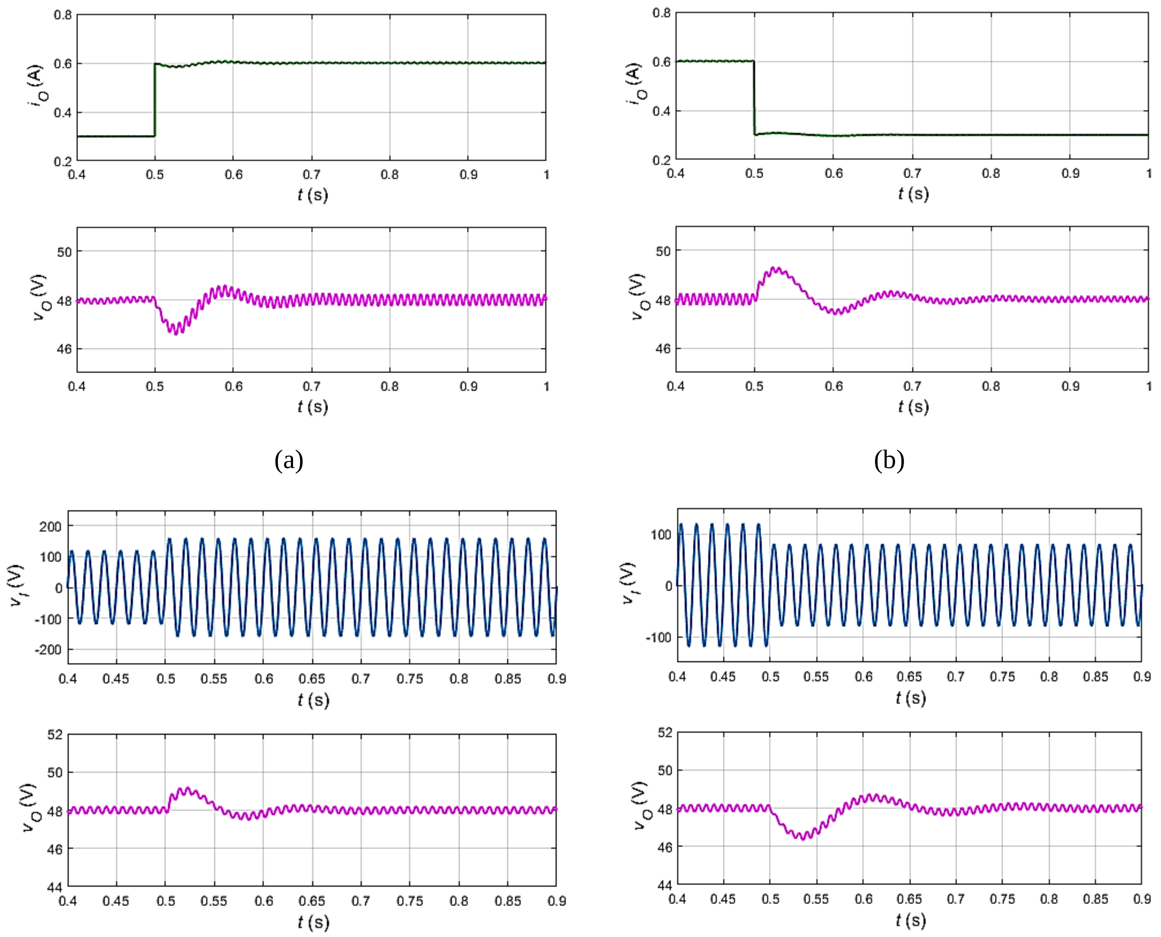

(a) (b)

(c) (d)

Figure 4. The response when i_O (a) increases from 0.3 A to 0.6 A and (b) decreases from 0.6 A to 0.3 A. The response when v_I (c) increases from 120 V to 160 V and (d) decreases from 120 V to 80 V

As for boost mode, Figures 5(a) and 5(b) show the transient response under load disturbance, whereas Figures 5(c) and 5(d) show the output voltage response under line disturbance. Obviously, Table 2 shows that the largest percentage undershoot has occurred during abrupt increase in load current and abrupt decrease in line voltage, which was around 3.6%. The longest settling time was 250 ms, which has occurred during abrupt decrease in load current. It can be observed that the line and load disturbances are rejected, while the output voltage is maintained at 220 VDC.

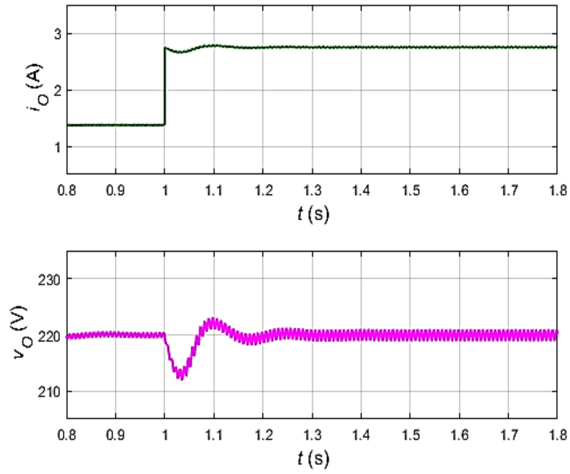

(a)

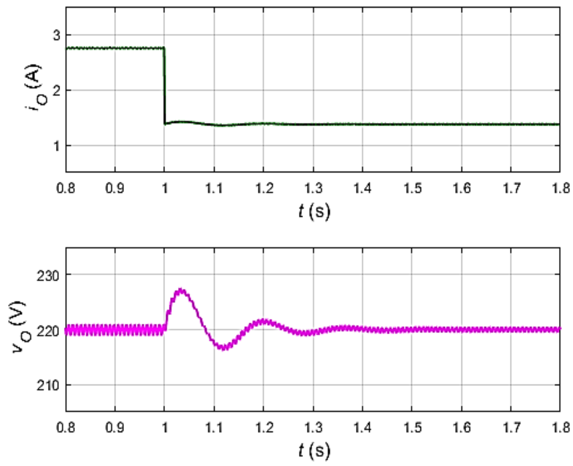

(b)

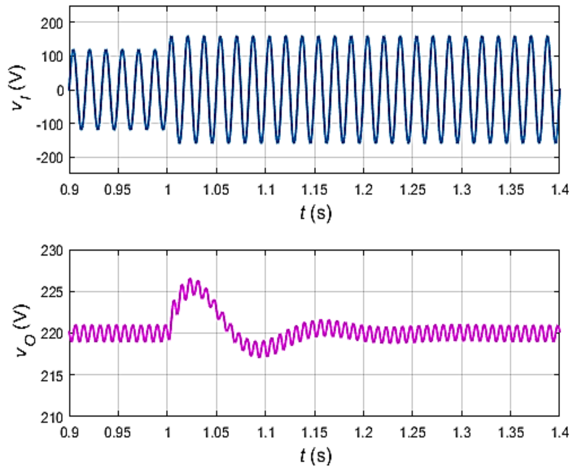

(c)

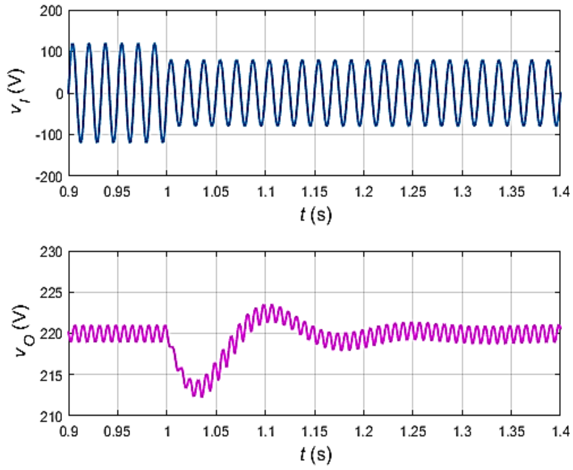

(d)

Figure 5. The response when i_O (a) increases from 1.37 A to 2.75 A and (b) decreases from 2.75 A to 1.37 A. The response when v_I (c) increases from 120 V to 160 V and (d) deceases from 120 V to 80 V

4.3. Comparison with conventional PI controller

A comparison is conducted between the proposed current-mode control and the conventional voltage-mode (PI) control of bridgeless single-switch AC-DC SEPIC converter during line and load disturbances. The control equations of the proposed u and voltage-mode u^* controllers are defined in (8) and (9), respectively.

$$u = 0.015(V_r - \beta v_o) + 1.45\int (V_r - \beta v_o)dt - 0.042\left|i_{L_I}\right| \tag{8}$$

$$u^* = 0.0009(V_r - \beta v_o) + 0.2\int (V_r - \beta v_o)dt. \tag{9}$$

The parameters of the conventional PI controller of bridgeless power converter are selected based on Ziegler-Nichols method for buck and boost operation. Figures 6(a) and 6(b) show response of the proposed and conventional voltage-mode controllers of the AC-DC power converter in buck mode, whereas Figure 6(c) and Figure 6(d) show the response of the two controllers in boost mode. It can be noticed that the output voltage response of the proposed control method produces faster transient response and lower percentage overshoot as compared to the conventional voltage-mode controller.

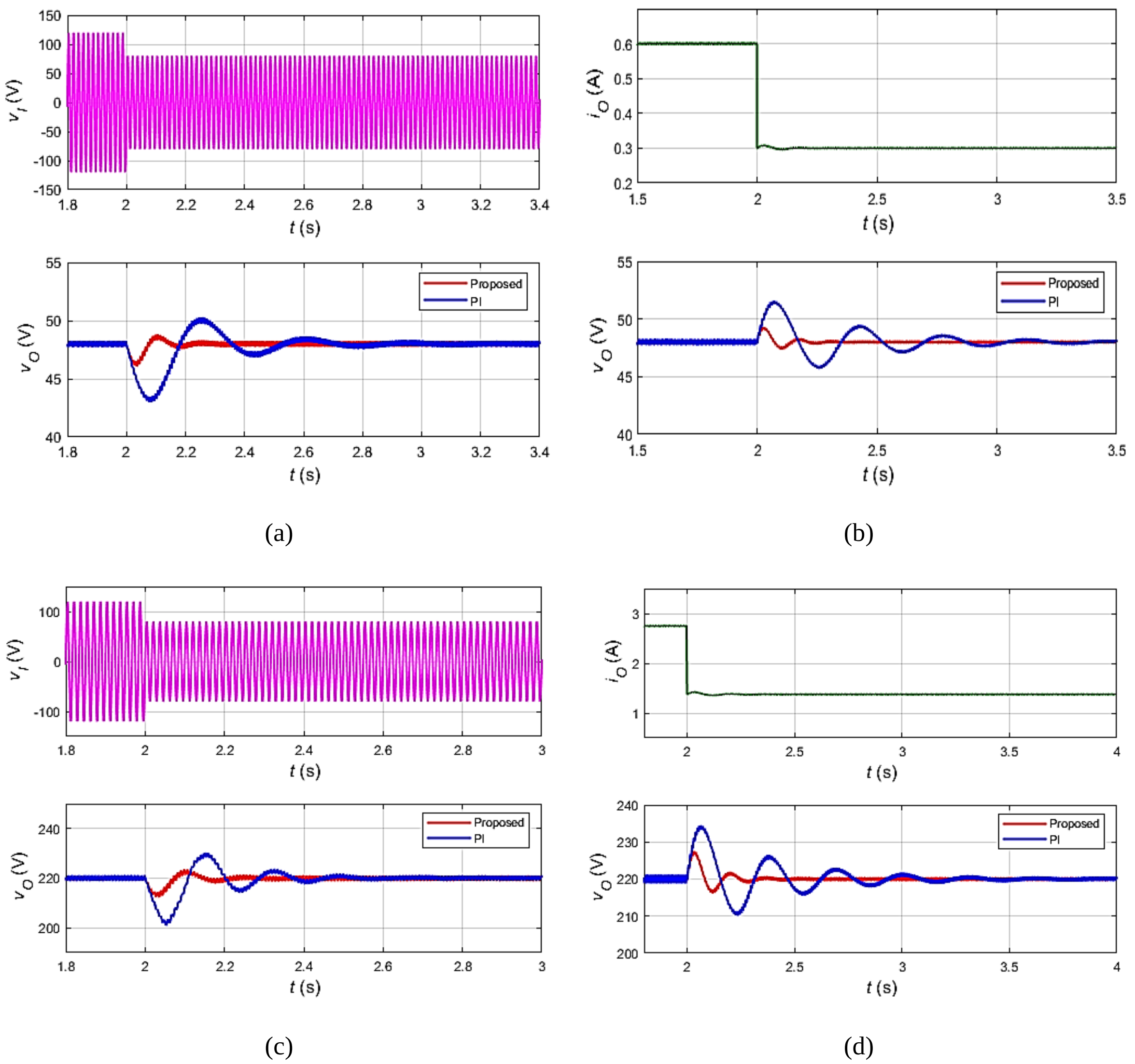

Figure 6. The operation of the proposed and PI controllers in buck mode during a step change in (a) v_I and (b) i_O. The operation of the proposed and PI controllers in boost mode during a step change in (c) v_I and (d) i_O

5. CONCLUSION

A large-signal model of a bridgeless SEPIC PFC converter has been developed. Further, a new control system has been designed to track the desired reference voltage under large disturbances in buck and boost modes. The proposed control method has a simple structure with minimal added components, which reduces the cost and complexity of the control scheme. The single-switch typology of the bridgeless AC-DC SEPIC converter also simplifies the gate driver circuitry and reduces the conduction loss. MATLAB simulation results have shown that the proposed current-mode controller provides enhanced transient response, robust tracking performance, and wide operating range.

ACKNOWLEDGEMENTS

The authors thank the department of electrical engineering at Wright State University for providing resources and technical support to accomplish this research endeavor.

REFERENCES

[1] Z. Zhang *et al*., "Analysis and design of a single-stage bridgeless isolated AC-DC resonant converter for programmable AC power source applications," in *IEEE Access*, vol. 8, pp. 219071–219082, 2020, doi: 10.1109/ACCESS.2020.3042541.

[2] R. Sasikala, and R. Seyezhai, "Review of AC-DC power electronic converter topologies for power factor correction," *International Journal of Power Electronics and Drive System (IJPEDS)*, vol. 10, no. 3, pp. 1510–1519, Sep. 2019, doi: 10.11591/ijpeds.v10.i3.pp1510-1519.

[3] F. Ferdous, and A. B. M. Harun-ur-Rashid, "Design of a high performance AC-DC LED driver based on SEPIC topology," *International Journal of Power Electronics and Drive System (IJPEDS)*, vol. 12, no. 2, pp. 870–885, Jun 2021, doi: 10.11591/ijpeds.v12.i2.pp870-885.

[4] S. M. Antony, and G. Immanuel, "A novel single phase bridgeless AC/DC PFC converter for low total harmonics distortion and high power factor," *International Journal of Power Electronics and Drive System (IJPEDS)*, vol. 9, no. 1, pp. 17–24, March 2018, doi: 10.11591/ijpeds.v9.i1.pp17-24.

[5] G. Li, J. Xia, K. Wang, Y. Deng, X. He, and Y. Wang, "A single-stage interleaved resonant bridgeless boost rectifier with high-frequency isolation," in *IEEE J. Emerg. Sel. Top. Power Electron*., vol. 8, no. 2, pp. 1767–1781, June 2020, doi: 10.1109/JESTPE.2019.2912434.

[6] H. Valipour, M. Mahdavi, and M. Ordonez, "Resonant bridgeless AC/DC rectifier with high switching frequency and inherent PFC capability," in *IEEE Transactions on Power Electronics*, vol. 35, no. 1, pp. 232–246, Jan. 2020, doi: 10.1109/TPEL.2019.2910755.

[7] W. M. Utomo *et al*., "Voltage tracking of bridgeless PFC Cuk converter using PI controller," *International Journal of Power Electronics and Drive System (IJPEDS)*, vol. 11, no. 1, pp. 367–373, March 2020, doi: 10.11591/ijpeds.v11.i1.pp367-373.

[8] H. Al-Baidhani, M. K. Kazimierczuk and A. Reatti, "Modeling and control of bridgeless single-switch non-inverting AC-DC Cuk converter in DCM," *IECON 2022 – 48th Annual Conference of the IEEE Industrial Electronics Society*, 2022, pp. 1-6, doi: 10.1109/IECON49645.2022.9968417.

[9] E. H. Ismail, "Bridgeless SEPIC rectifier with unity power factor and reduced conduction losses," in *IEEE Transactions on Industrial Electronics*, vol. 56, no. 4, pp. 1147–1157, April 2009, doi: 10.1109/TIE.2008.2007552.

[10] M. Mahdavi, and H. Farzanehfard, "Bridgeless SEPIC PFC rectifier with reduced components and conduction losses," in *IEEE Transactions on Industrial Electronics*, vol. 58, no. 9, pp. 4153–4160, Sept. 2011, doi: 10.1109/TIE.2010.2095393.

[11] J. Yang, and H. Do, "Bridgeless SEPIC converter with a ripple-free input current," in *IEEE Transactions on Power Electronics*, vol. 28, no. 7, pp. 3388–3394, July 2013, doi: 10.1109/TPEL.2012.2226607.

[12] A. J. Sabzali, E. H. Ismail, M. A. Al-Saffar, and A. A. Fardoun, "New bridgeless DCM SEPIC and Cuk PFC rectifiers with low conduction and switching losses," in *IEEE Transactions on Industry Applications*, vol. 47, no. 2, pp. 873–881, March-April 2011, doi: 10.1109/TIA.2010.2102996.

[13] B. Singh, and R. Kushwaha, "A PFC based EV battery charger using a bridgeless isolated SEPIC converter," in *IEEE Transactions on Industry Applications*, vol. 56, no. 1, pp. 477–487, Jan.-Feb. 2020, doi: 10.1109/TIA.2019.2951510.

[14] A. M. Al Gabri, A. A. Fardoun, and E. H. Ismail, "Bridgeless PFC-modified SEPIC rectifier with extended gain for universal input voltage applications," in *IEEE Transactions on Power Electronics*, vol. 30, no. 8, pp. 4272–4282, Aug. 2015, doi: 10.1109/TPEL.2014.2351806.

[15] S. Singh, B. Singh, G. Bhuvaneswari, and V. Bist, "A power quality improved bridgeless converter-based computer power supply," in *IEEE Transactions on Industry Applications*, vol. 52, no. 5, pp. 4385–4394, Sept.-Oct. 2016, doi: 10.1109/POWERI.2014.7117749.

[16] P. J. S. Costa, C. H. Illa Font, and T. B. Lazzarin, "Single-phase hybrid switched-capacitor voltage-doubler SEPIC PFC rectifiers," in *IEEE Transactions on Power Electronics*, vol. 33, no. 6, pp. 5118–5130, June 2018, doi: 10.1109/TPEL.2017.2737534.

[17] H. Ma, Y. Li, J. Lai, C. Zheng, and J. Xu, "An improved bridgeless SEPIC converter without circulating losses and input-voltage sensing," in *IEEE Journal of Emerging and Selected Topics in Power Electronics*, vol. 6, no. 3, pp. 1447–1455, Sept. 2018, doi: 10.1109/JESTPE.2017.2768545.

[18] N. A. Rail, M. J. Abdul Aziz, and M. R. Sahid, "Bridgeless PFC single ended primary inductance converter in continuous current mode," *International Journal of Power Electronics and Drive System (IJPEDS)*, vol. 10, no. 3, pp. 1427–1436, Sep. 2019, doi: 10.11591/ijpeds.v10.i3.pp1427-1436.

[19] R. M. Devi, and L. Premalatha, "Soft computing technique of bridgeless SEPIC converter for PMBLDC motor drive," *International Journal of Power Electronics and Drive System (IJPEDS)*, vol. 9, no. 4, pp. 1503–1509, Dec. 2018, doi: 10.11591/ijpeds.v9.i4.pp1503-1509.

[20] Y. Liu, X. Huang, Y. Dou, Z. Ouyang, and M. A. E. Andersen, "GaN-based ZVS bridgeless dual-SEPIC PFC rectifier with integrated inductors," in *IEEE Transactions on Power Electronics*, vol. 36, no. 10, pp. 11483–11498, Oct. 2021, doi: 10.1109/TPEL.2021.3070961.

[21] J. Gupta, and B. Singh, "Single stage isolated bridgeless charger for light electric vehicle with improved power quality," *IEEE International Conference on Power Electronics Drives and Energy Systems (PEDES)*, 2020, pp. 1-6, doi: 10.1109/PEDES49360.2020.9379852.

[22] P. F. de Melo, R. Gules, E. F. R. Romaneli, and R. C. Annunziato, "A modified SEPIC converter for high-power-factor rectifier and universal input voltage applications," in *IEEE Transactions on Power Electronics*, vol. 25, no. 2, pp. 310–321, Feb. 2010, doi: 10.1109/TPEL.2009.2027323.

[23] Y. Onal, and Y. Sozer, "A new single switch bridgeless SEPIC PFC converter with low cost low THD and high PF," *2015 9th International Conference on Electrical and Electronics Engineering (ELECO)*, 2015, pp. 649-653, doi: 10.1109/ELECO.2015.7394472.

[24] E. Madrid, D. Murillo-Yarce, C. Restrepo, J. Muñoz, and R. Giral, "Modelling of SEPIC, Ćuk and Zeta converters in discontinuous conduction mode and performance evaluation," *Sensors, vol. 21, no. 22,* 2021, doi: 10.3390/s21227434.

[25] H. Al-Baidhani, and M. K. Kazimierczuk, "Simplified double-integral sliding-mode control of PWM DC-AC converter with constant switching frequency," *Applied Sciences*, vol. 12, no. 20, p. 10312, Oct. 2022, doi: 10.3390/app122010312.

[26] H. Al-Baidhani, T. Salvatierra, R. Ordóñez and M. K. Kazimierczuk, "Simplified nonlinear voltage-mode control of PWM DC-DC buck converter," in *IEEE Transactions on Energy Conversion*, vol. 36, no. 1, pp. 431-440, March 2021, doi: 10.1109/TEC.2020.3007739.

[27] H. Komurcugil, S. Biricik and N. Guler, "Indirect sliding mode control for DC–DC SEPIC converters," *IEEE Trans. Ind. Informatics*, vol. 16, no. 6, pp. 4099-4108, Jun. 2020, doi: 10.1109/TII.2019.2960067.

[28] B. A. Martínez-Treviño, A. E. Aroudi, A. Cid-Pastor, G. Garcia, and L. Martinez-Salamero, "Synthesis of constant power loads using switching converters under sliding-mode control," in *IEEE Transactions on Circuits and Systems I: Regular Papers*, vol. 68, no. 1, pp. 524-535, Jan. 2021, doi: 10.1109/TCSI.2020.3031332.

BIOGRAPHIES OF AUTHORS

Humam Al-Baidhani received the B.Sc. degree in electrical engineering and the M.S. degree in electrical power engineering, both from University of Technology in Baghdad, Iraq, in 2008 and 2011, respectively; and the Ph.D. degree in electrical engineering from Wright State University in Ohio, USA, in 2020. He was a Graduate Teaching and Research Assistant of electrical engineering at Wright State University from 2018–2020. He is currently with the Department of Computer Techniques Engineering, Imam Ja'afar Al-Sadiq University, Iraq. His research interests include power converters, modeling and control, nonlinear systems, and power systems stability. He can be contacted at email: humam@sadiq.edu.iq.

Abdullah Sahib Abdulsada received the B.Sc. degree in electrical engineering, the M.S. degree in electrical power engineering, and the Ph.D. degrees in electrical power engineering from University of Technology in Baghdad, Iraq, in 1993, 2010, and 2018, respectively. He is currently with the Department of Electronic and Communication Technologies, Al-Furat Al-Awsat Technical University, Iraq. His research interests include power electronics, renewable energy, and electrical power systems. He can be contacted at email: abdward780@atu.edu.iq.